

# Optical properties of atmospheric aerosols over the Arabian Sea and Indian Ocean: North-south contrast across the ITCZ

K. Krishna Moorthy\*, Auromeet Saha<sup>‡</sup>, K. Niranjan<sup>‡</sup> and Preetha S. Pillai\*

\*Space Physics Laboratory, Vikram Sarabhai Space Centre, Thiruvananthapuram 695 022, India

<sup>‡</sup>Department of Physics, Andhra University, Visakhapatnam 530 003, India

Extensive estimates of aerosol spectral optical depths are made over the Arabian Sea and south-western Indian Ocean, using a 10-channel multi-wavelength solar radiometer (MWR) and a 4-channel hand held EKO sun-photometer (ESP) on-board the cruise # 133 of ORV *Sagar Kanya* during the First Field Phase (FFP-98) of the Indian Ocean experiment (INDOEX) in February and March 1998. High values of optical depths, particularly in the visible wavelengths, are encountered in the coastal areas, with a gradual increase from Goa to Male. The optical depths decrease sharply as the ship moves out to the south-western Indian Ocean across the equator; the effect is more significant at shorter wavelengths. Over the pristine environment south of the ITCZ, extremely low optical depths appear at the visible wavelengths, while at the NIR wavelengths, the optical depths remain nearly the same as on the northern side. On the return leg, again higher optical depths are encountered north of the ITCZ with those at the visible wavelengths sharply increased. Over the north-western Arabian Sea, higher optical depth values occur farther away from the coast, suggesting additional input of aerosols over mid ocean, possibly transported by various wind trajectories from the west Asian deserts. Comparing air trajectories both at the surface and 850 hPa reveals that in addition to those advected from continental India, winds transporting aerosols from various north/west Asian regions contribute significantly to the aerosol optical depths over the Arabian Sea.

STUDIES of marine aerosols are important because of their direct and indirect interaction with the incoming solar and outgoing terrestrial radiations<sup>1-3</sup>. In addition, aerosols can significantly modify ocean visibility. Marine aerosols are mainly composed of the following: (i) sea-salt aerosols produced over the sea surface by wind<sup>4-8</sup>, (ii) non-sea salt aerosols produced mainly by the photolytic decomposition of dimethyl sulphide (DMS) emitted by marine phytoplankton<sup>9-11</sup> and (iii) continental components (both of

natural and anthropogenic origin) advected by offshore winds<sup>12-14</sup>. All these processes are quite significant over the tropical oceanic regions adjoining India, though the aerosol properties over these regions are not thoroughly explored<sup>15</sup>. The Indian Ocean Experiment (INDOEX) aims at assessing both the role of continental aerosols in influencing the radiative forcing over oceans and also the role of seasonally changing ITCZ (Inter-Tropical Convergence Zone) in transporting the continental aerosols to pristine oceanic environments<sup>13</sup>. Several co-ordinated cruise and ground-based measurements have been conducted as part of the INDOEX to characterize aerosols over the tropical Indian Ocean and to study their N-S gradients<sup>16,17</sup>. However these studies have been mainly confined to the tropical Indian Ocean regions, and no measurements could be made due south of the ITCZ, in the so-called pure and pristine oceanic environment. The First Field Phase (FFP) of the INDOEX was mainly planned to fill this gap, and aerosol properties were extensively measured across the ITCZ. This paper presents the details of the measurements of aerosols optical properties on-board a scientific cruise during the FFP of INDOEX. The results are discussed.

## The cruise and the experiments

The scientific cruise # 133 ORV *Sagar Kanya* has been dedicated to the FFP-98 of the INDOEX. The 42-day cruise, started from Goa on 18 February 1998 and returned after the experiments on 31 March 1998; Figure 1 shows the trajectory, with circles denoting the daily position of the ship at ~ 1130 UT and corresponding dates given as well, starting from February 18. The ship, moved nearly parallel initially to the western coast of India, had two 1-day stoppages: at first near Thiruvananthapuram (TVM) on 22 February, and then near Minicoy on 23 February 1998. Simultaneous ground-based measurements were undertaken using complementary instruments on the land. The ship also had port-calls at Male (25 to 28 February) and at Port Louis, Mauritius (12 to 16 March 1998).

\*For correspondence. (e-mail: spl\_vssc@vssc.org)

The aerosol measurements reported in this paper are spectral optical depths estimated at a number of narrow wavelength bands in the visible and near infrared region using a 10-channel multiwavelength solar radiometer (MWR)<sup>16</sup> and a 4-channel commercial hand held sun-photometer (ESP, model MS-120 of EKO, Japan). The important specifications of both these instruments are given in Table 1. The instruments were operated on-board the cruise when unobstructed sunshine was available for at least 2 hours. However, due to some technical snags, the MWR observations commenced only on 25 February 1998. The dates when at least one of the instruments was operating are identified by filled circles on the cruise track in Figure 1; open circles signify, cloudy/overcast days when radiometer observations were impossible.

### Analysis of data and intercomparison of optical depths

From the spectral extinction measurements made using the MWR and the ESP, aerosol spectral optical depths ( $\tau_{p\lambda}$ ) are estimated following the Langley technique<sup>16,18</sup>. Data obtained on any single day are considered as single set, and the retrieved  $\tau_{p\lambda}$  corresponds to the mean value for that day. The number of observation points in each data set varied from about 10 to as much as 40 depending on the duration of observation and the stability of the ship (e.g. data collection was more time consuming when positioning instruments aligned with the sun during rough

seas). The observation points were generally higher for ESP. In addition, the regression that fits to the data points is by and large very good, and the scatter of the measurement points from the fitted lines is very small, thereby indicating that the experiment has been carried out with proper care.

As seen in Table 1, both the MWR and ESP have one wavelength in common: 500 nm. As such, an intercomparison between the  $\tau_p$  values estimated using both these instruments has been made, primarily to assess the quality, reliability and reproducibility of the data. This was done in three stages. Before the cruise these instruments were operated simultaneously on 4 days at TVM during a pre-INDOEX intercomparison campaign<sup>19</sup>. During the cruise simultaneous data were obtained over 14 days and after the cruise over two days in April 1998. The result is shown in Figure 2 with the individual points corresponding to  $\tau_{p\lambda}$  from each set of observations and the orthogonal bars, the respective total errors. The dashed line represents the ideal scenario when both the instruments yield identical  $\tau_p$  values. Clearly in Figure 2 the experimental points fall closely about the ideal line

Table 1. Specifications of MWR and ESP

Parameter	MWR	ESP
No. of channels	10	4
Centre wavelengths (nm)	380, 400, 450, 500, 600, 650, 750, 850, 935 and 1025	366, 500, 675 and 778
Bandwidth (full width at half maximum - nm)	6 to 10	5 to 6
Field of view	2.1°	2.4°
Operation	on ground/deck	Hand held
Detection	~ 1 sec average at the peak	peak
Time constant (s)	1	2

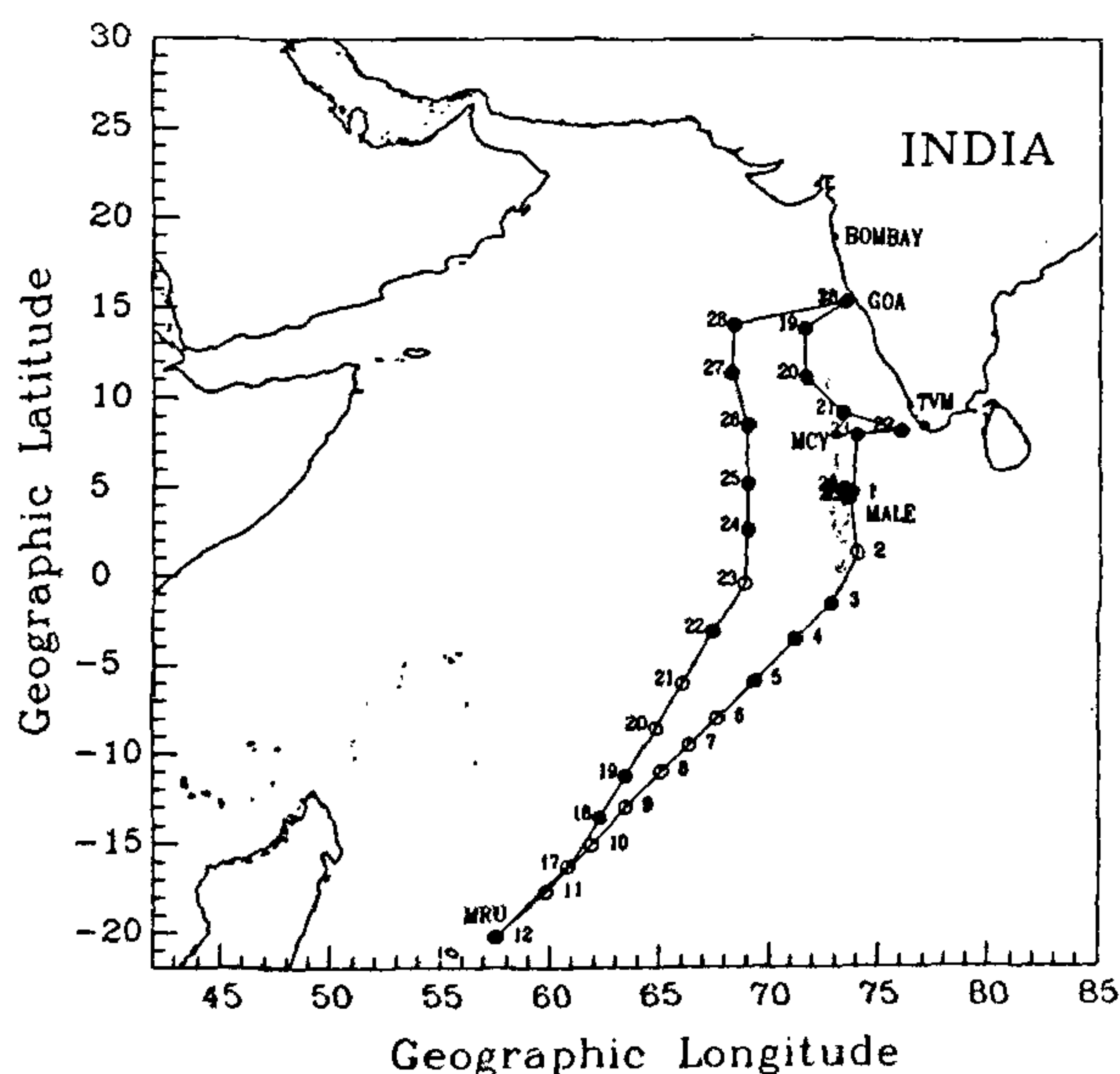


Figure 1. The cruise track of ORV Sagar Kanya during the FFP with the circles showing the daily positions. The filled circles show the days when  $\tau_p$  data are available (either from MWR or ESP).

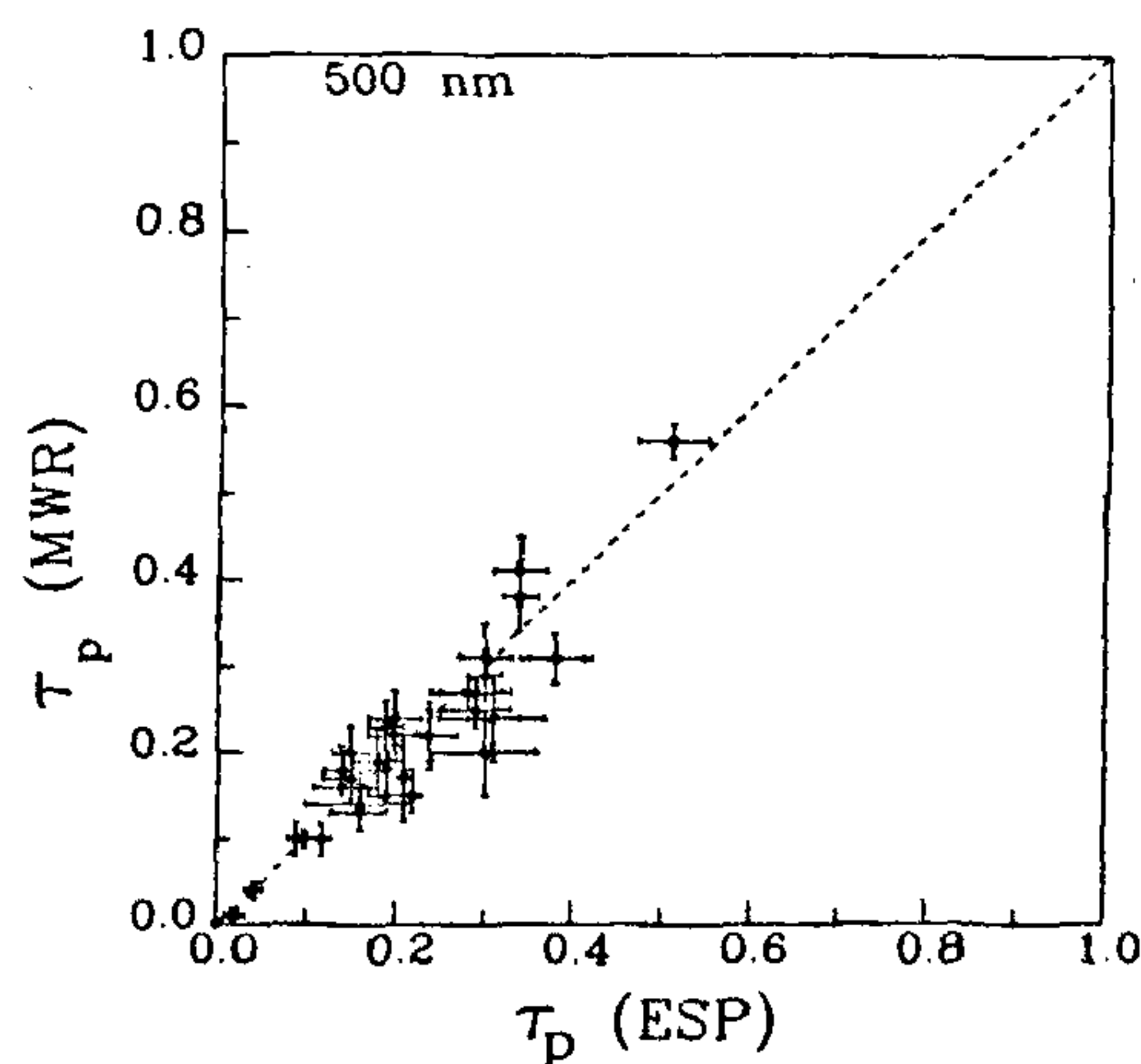


Figure 2. Intercomparison of  $\tau_p$  values at 500 nm between those deduced from the MWR and those deduced from ESP. The bars through the points are the respective errors.

generally and on the line on several instances, with a correlation coefficient better than 0.9; thus both the instruments are complementary in nature and data from either of them can be used to describe the aerosol optical characteristics with the same degree of accuracy.

### Supplementary data

Besides the aerosol spectral optical depths estimated above, other data describing the general state of the atmosphere have been obtained from the various instruments on-board the *Sagar Kanya*. These included regular values of wind speed ( $U \text{ ms}^{-1}$ ), direction ( $\theta^\circ$  clockwise w.r.t to north), relative humidity (RH%), ambient air temperature ( $t^\circ\text{C}$ ) and pressure ( $P$ , hPa) all measured at the deck level,  $\sim 10$  m above the water level. These values are generally available at every 10-min interval along with the instantaneous ship position in latitude and longitude, and these formed the supplementary data. The wind speed and direction are corrected for the ship's velocity and only the true values are used in this study.

### Results

#### Chronological variation of parameters

Chronological variations of some of these parameters are shown along with those of  $\tau_p$  at 500 nm in Figure 3 where

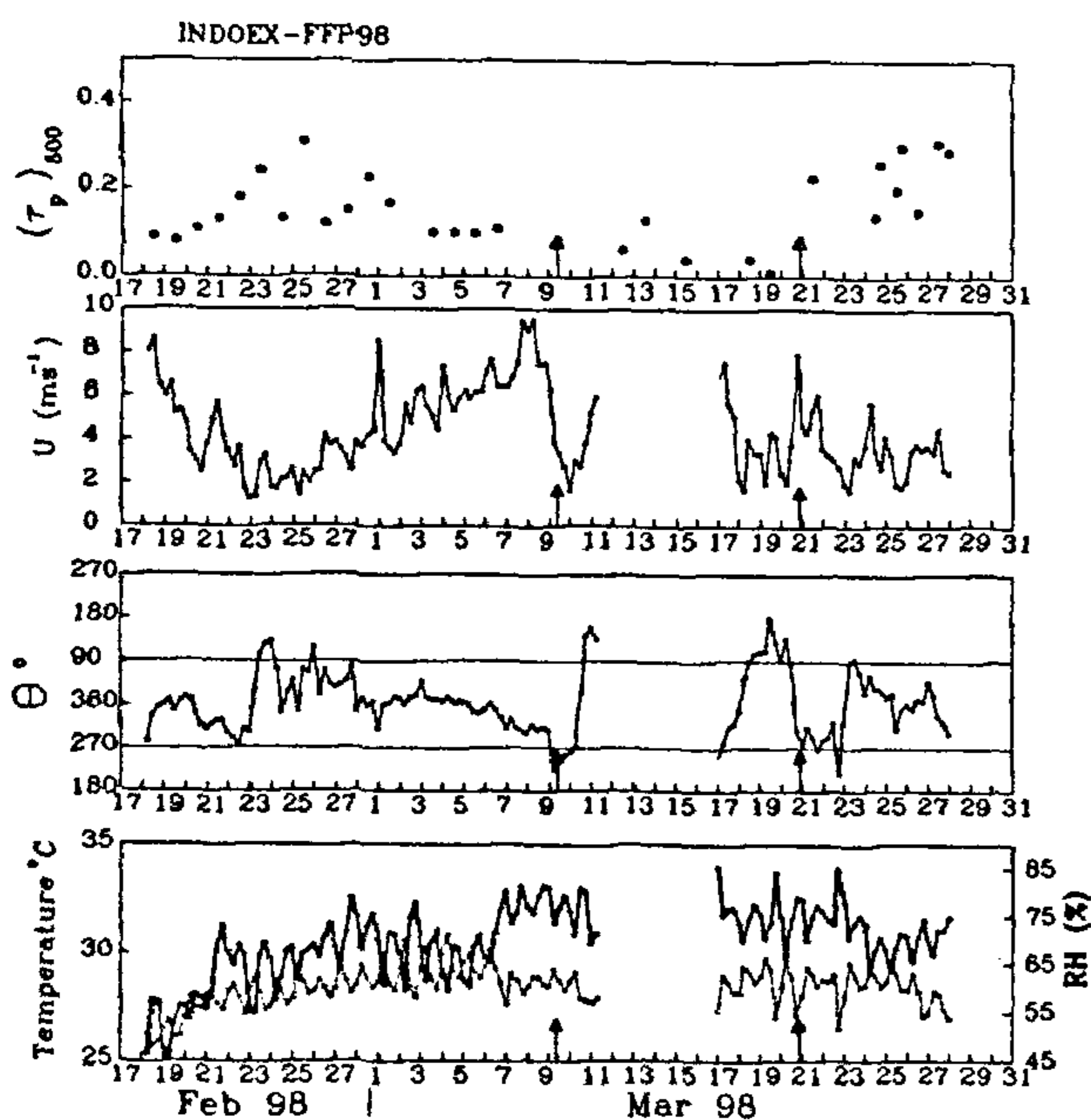


Figure 3. Chronological variation of aerosol optical depth along with the corresponding atmospheric parameters. The different panels from top to bottom show the variations of  $\tau_p$  at 500 nm (top most), wind speed (second from top), wind direction (second from bottom) and RH and  $t$  (bottom most) respectively.

the panels from the top to the bottom show variations of  $\tau_p$ ,  $U$ ,  $\theta$  and RH and  $T$  (dashed line). The two dashed horizontal lines in the  $\theta$  panel are drawn such that the directions lying between them represent winds directed from the northern hemisphere and blowing towards the south while those outside represent the reverse flow pattern. The  $\tau_p$  values are the mean value for the observation day, while all the rest are 6 hourly mean values. We also see that the cruise period has been generally free from any major weather phenomenon. The mean wind has been generally low to moderate with speeds in the range 3 to  $6 \text{ ms}^{-1}$ , except from 6 to 8 March 1998 when values exceeding  $6 \text{ ms}^{-1}$  occurred for two days. Winds have been generally directed from N-W, N, N-E until 9 March 1998 and from 21 March 1998 as shown by the variations of  $\theta$ . RH shows a gradual increase from  $\sim 55\%$  near the coast to  $\sim 80\%$  over mid-ocean. There is a sudden change or discontinuity in the variations of these parameters with  $U$  becoming the lowest, a sudden reversal in  $\theta$  from northerly to southerly and a decrease in  $T$ , all occurring simultaneously around 9 March on the onward leg and 21 March during the return leg. These changes are associated with the ship crossing the ITCZ where the two opposing (northerly and southerly) winds converge, leading to deep convections. The winds are S-W, S, S-E due south of this and from the north due north. The vertical arrows on the abscissa in Figure 3 indicate the position of the ITCZ; these positions were later confirmed by the India Meteorological Department.

The aerosol optical depth (at 500 nm) in the top panel shows a gradual increase along the coast from Goa to Minicoy (18 to 23 February 1998) and then slowly decreases as the ship reaches Male on 25 February 1998. Over the Indian Ocean,  $\tau_p$  decreases rapidly as ship moves out of Male on 1 March towards the ITCZ. Around the ITCZ region the sky was cloudy and no observations were possible from 6 March till the ship reached Port Louis, (Mauritius, MRU) on 12 March 1998. During 9 March to 20 March, when the ship was in the ocean south of the ITCZ, aerosol optical depths were extremely low values as seen in Figure 3 (top panel) between the two arrows. Such low values of  $\tau_p$  (at 500 nm) are rare in the northern hemisphere and in the long period data available at ground stations like TVM. In the return leg, high values of  $\tau_p$  occur again north of the ITCZ from 23 March onwards once the ship crosses the cloudy region around the ITCZ.

#### Spatial picture

Using the  $\tau_p$  values at 500 nm and the corresponding position co-ordinates of the ship, a spatial mosaic of  $\tau_p$  is constructed over the oceanic area of investigation. In Figure 4, on the map of the region, the vertical bars indicate the value of  $(\tau_p)_{500}$ , with their heights proportional to

the  $\tau_p$  values. The height of the bar for  $\tau_p = 0.2$  appears on the right top corner of the figure. The dashed horizontal lines mark the positions of the ITCZ with the one towards farther south indicating the position during the onward leg. During the return leg ITCZ moved  $\sim 5^\circ$  further to the north, occurring at  $\sim 5$  to  $6^\circ$  S (ref. 15). The  $\tau_p$  values obtained from MWR observations from TVM on 22 February 1998 and from Minicoy (MCY) on 23 February 1998 are also included in Figure 4. During that period, *Sagar Kanya* stopped at  $\sim 100$  km offshore from these locations, and synchronous observations are made on-shore and on-board. It is evident from Figure 4 that the optical depth is generally high over the entire west coast of India (higher overland) and gradually increases N-S, even though the southern coastal regions are not increasingly industrialized. However, as one moves farther away from the Indian peninsula into remote oceanic regions,  $\tau_p$  decreases gradually. Nevertheless the  $\tau_p$  values remain moderately high over the entire regions on the northern side of the ITCZ (including regions south of the equator, but north of ITCZ). However, the southern regions of the ITCZ reveal a rather cleaner and purer environment with very low values of optical depth over the ocean as well as at Port Louis. In contrast, over the Arabian Sea, on the return leg, higher optical depths are encountered north of the ITCZ and the equator over oceanic regions farther away from the coast than at regions closer to the Indian coast. Normally one would expect higher  $\tau_p$  values closer to the coast, due to the proximity to the potentially strong source regions over the continents. Over the ocean, these aerosols are usually removed from the atmosphere by sedimentation and precipitation and with weaker input

from oceans (as winds are weaker  $\leq 4 \text{ ms}^{-1}$ , Figure 3)  $\tau_p$  is expected to decrease to remote oceanic regions. Thus the increase in  $\tau_p$  along N-S close to the coast and E-W across the coast are indicative of possible transport of aerosols by discrete air trajectories. This aspect is examined further in a companion paper<sup>20</sup>.

### Spectral variations

The spectral variations are examined by plotting  $\tau_{p\lambda}$  against  $\lambda$  in Figure 5 where the top and bottom panels represent the scenario north of ITCZ (onward and return legs) in contrast with that on the south of the ITCZ shown in the middle panel. A drastic reduction in  $\tau_p$  occurs at wavelengths on the shorter side of 650 nm on the south while on the longer wavelength side the optical depths are comparable in all the three cases. Moreover, in the top and bottom panels,  $\tau_p$  decreases from a high value at the shortest wavelength initially faster and then more gradually, whereas on the south of the ITCZ,  $\tau_p$  is extremely

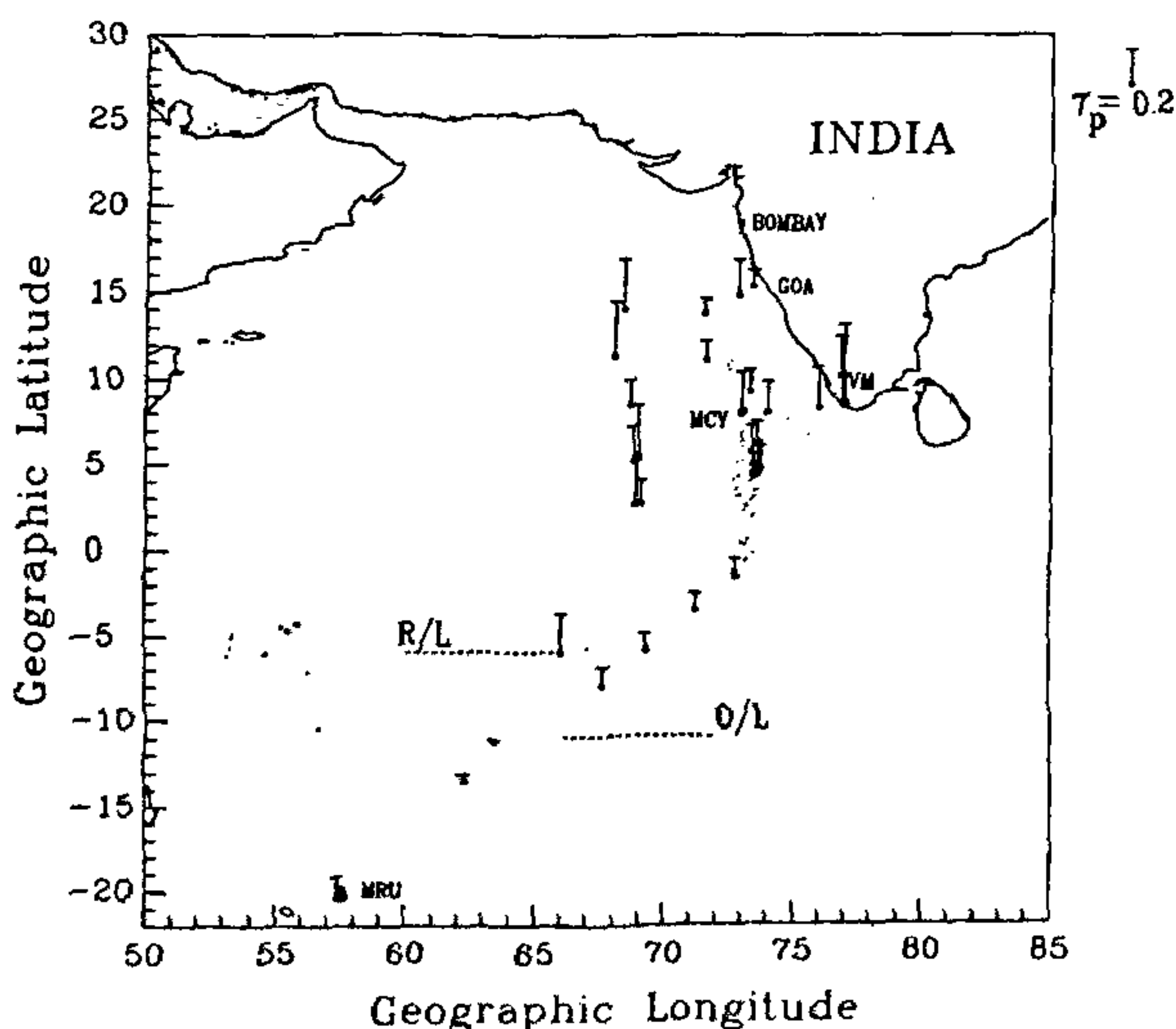


Figure 4. Spatial mosaic of  $(\tau_p)_{500}$  over the Arabian Sea and Indian Ocean during the FFP. Data from ground observations at TVM and Minicoy are also included.

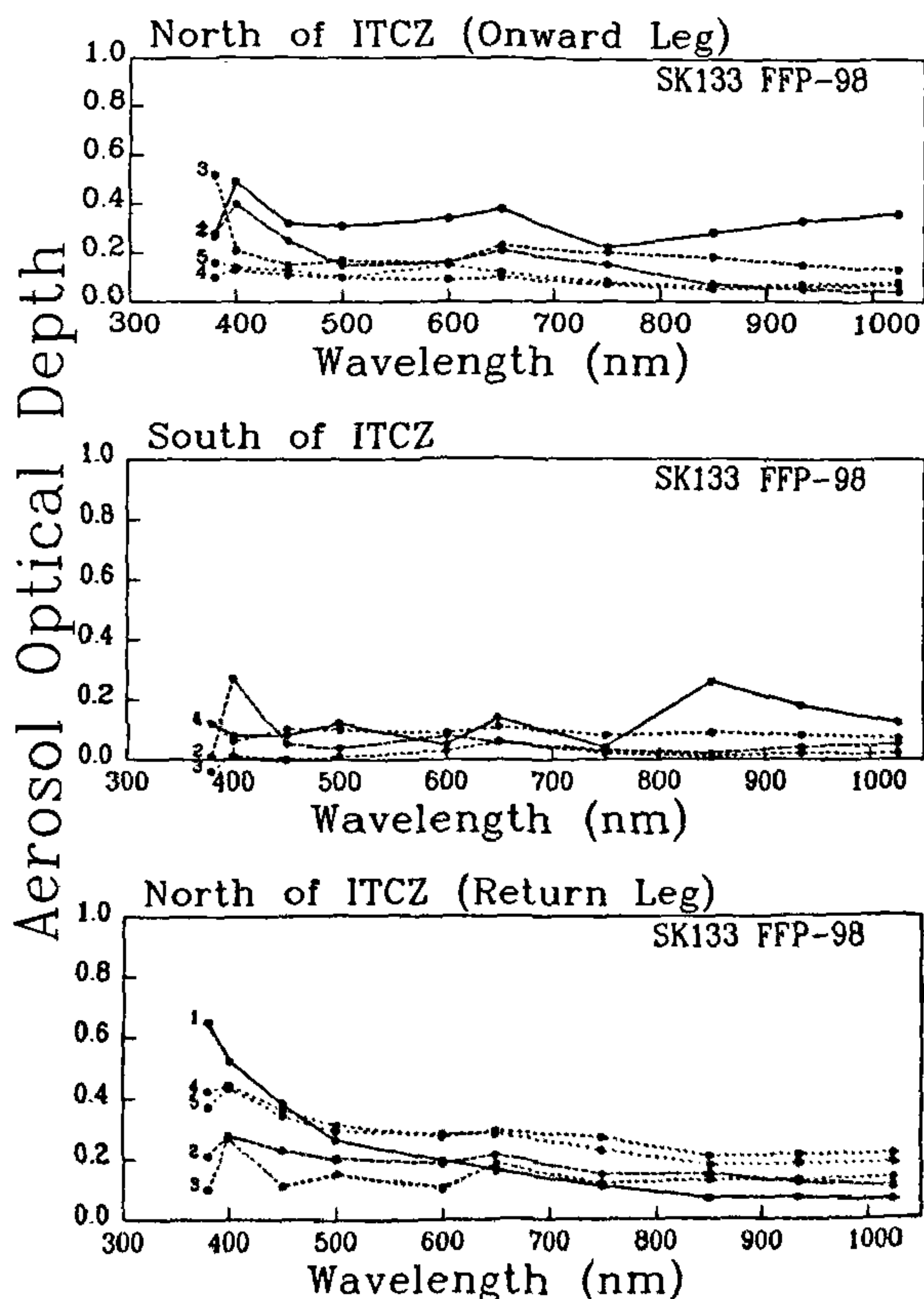


Figure 5. Spectral variation of  $\tau_{p\lambda}$ . Panels from top to bottom show the scenario on the north of the ITCZ (onward leg), on the south of the ITCZ and on the north of the ITCZ (return leg). Note the dramatic increase in  $\tau_p$  at  $\lambda < 700$  nm in the top and bottom panels. (The numbers on the left of the curves in each panel correspond to data obtained on different days.)

low and nearly wavelength-independent in the visible region; it then increases slowly at longer wavelengths. The theory of Mie scattering demonstrates that maximum contribution to scattering/extinction at a given wavelength  $\lambda$  arises from particles with diameters in the range  $\lambda/2$  to  $\lambda$ . Viewed in this perspective the above observation indicates a sharp decrease in the concentration of submicron aerosols in the marine atmosphere from N-S across the ITCZ. However, a quantitative analysis of this is possible only if the aerosol size distributions and other size parameters representing the aerosol characteristics are known. This aspect is dealt with in detail in a companion paper in this issue<sup>20</sup>.

### Summary and conclusions

The investigation of aerosol optical properties over Indian Ocean across the ITCZ has revealed the following:

(1) Aerosol optical depths decrease towards remote oceanic regions farther away from the land.

(2) Close to the west coast of India, optical depths are quite large and show a gradual increase along the coast from N-S.

(3) Optical depths remain high/moderate over the entire oceanic region on the north of the ITCZ while optical depths are extremely low on the south of ITCZ, particularly at shorter wavelengths.

(4) Optical depths at the near IR wavelengths remain nearly the same throughout irrespective of the ITCZ, thereby showing them to be caused by larger aerosols of oceanic origin.

(5) Transport of aerosols from the west Asian deserts appears to cause increased aerosol loading in the central Arabian Sea, leading to an increase in optical depths with distance across the coast. The contribution due to this is comparable to or even more than due to the continental winds from India, over the coastal regions.

1. Charlson, R. J., Lovelock, J. E., Andreae, M. O. and Warren, S. G., *Nature*, 1987, 326, 655-661.

2. Fitzgerald, J. W., *Atmos. Environ. (Part A)*, 1991, 25, 533-545.
3. Ramanathan, V., Crutzen, P. J., Coakley, J. A., Clarke, A., Collins, W. D., Dickerson, R., Fahey, D., Gandrud, B., Heymsfield, A., Kiehl, J. T., Kuettner, J., Krishnamurti, T. N., Lubin, D., Maring, H., Ogren, J., Prospero, J., Rasch, P. J., Savoie, D., Shaw, G., Tuck, A., Valero, F. P. J., Woodbridge E. L. and Zhang, G., *Publication # 162*, Scripps Institution of Oceanography, UCSD, California, USA, 1996, pp. 1-83.
4. Woodcock, A. H., *J. Meteorol.*, 1953, 10, 362-371.
5. Lovett, R. F., *Tellus*, 1978, 30, 358-364.
6. Exton H. J., Latham, J., Park, P. M., Perry, S. J., Smith, M. H. and Allan, R. R., *Q. J. R. Meteorol. Soc.*, 1985, 111, 817-837.
7. Monahan, E. C., Spiel, D. E. and Davidson, K. L., *Oceanic Whitecaps*, Reidel, Hingham, MA, 1986.
8. O'Dowd, C. D. and Smith H., *J. Geophys. Res.*, 1993, 98, 1137-1149.
9. Hegg, D. A., Radke, L. F. and Hobbs, P. V., *J. Geophys. Res.*, 1991, 96, 18727-18733.
10. Quinn, P. K., Covert, D. S., Bates, T. S., Kapustin, V. N., Ramsey-Bell, D. C. and Mc Innes, L. M., *J. Geophys. Res.*, 1993, 98, 10411-10427.
11. Russell, L. M., Pandis, S. N. and Seinfeld, J. H., *J. Geophys. Res.*, 1994, 99, 20989-21003.
12. Prospero, J. M., *J. Geophys. Res.*, 1979, 84, 725-731.
13. Bergametti, G., Gomes, L., Coude-Gaussen, G., Rognon, P. and Le Couster, M. N., *J. Geophys. Res.*, 1989, 94, 14855-14864.
14. Tyson, P. D., Garstang, M., Swap, R., Kallberg, P. and Edwards, N., *Int. J. Climatol.*, 1996, 16, 256-291.
15. Jha, B. and Krishnamurti, T. N., Scientific Report, FSU 98-08, 1998.
16. Moorthy, K. K., Satheesh, S. K. and Murthy B. V. K., *J. Geophys. Res.*, 1997, 102, 18827-18842.
17. Satheesh, S. K., Moorthy, K. K. and Murthy, B. V. K., *J. Geophys. Res.*, 1998, 103, 26183-26192.
18. Satheesh, S. K. and Moorthy K. K., *Tellus*, 1997, 49B, 417-429.
19. Parameswaran, K., Moorthy, K. K. and Nair, P. R., Scientific Report, 1998, SPL: SR:002:98, Space Physics Laboratory, VSSC, Thiruvananthapuram.
20. Moorthy, K. K., Pillai, P. S., Saha, A. and Niranjan, K., *Curr. Sci.*, 1999 (this issue).

ACKNOWLEDGEMENTS. We thank the Department of Ocean Development and the National Institute of Oceanography for the ship board facilities. We thank B. V. Krishna Murthy, the then Director, SPL for encouragement and useful discussions. The help provided by K. Sindhu and the observers at Minicoy in collecting MWR data is also acknowledged.

# Aerosol size characteristics over the Arabian Sea and Indian Ocean: Extensive sub-micron aerosol loading in the northern hemisphere

K. Krishna Moorthy\*<sup>§</sup>, Preetha S. Pillai\*, Auromeet Saha<sup>#</sup> and K. Niranjana<sup>#</sup>

\*Space Physics Laboratory, Vikram Sarabhai Space Centre, Thiruvananthapuram 695 022, India

<sup>§</sup>Department of Physics, Andhra University, Visakhapatnam 530 003, India

Aerosol size characteristics and columnar loading are deduced from spectral optical depths estimated over the Arabian Sea and south-western Indian Ocean, using a 10 channel multi-wavelength solar radiometer (MWR) on board the cruise #133 of ORV *Sagar Kanya* during the First Field Phase (FFP-98) of the Indian Ocean Experiment (INDOEX). The columnar size distributions showed a clear and consistent bimodal nature over the oceanic areas of the northern hemisphere (or due north of the inter-tropical convergence zone (ITCZ)) with a sub-micron accumulation mode at  $\sim 0.05 \mu\text{m}$  and a coarse particle mode at  $\sim 1 \mu\text{m}$ ; both are attributed to different source mechanisms. There is a rapid decrease in aerosol mass loading as one moves to remote oceanic regions from the coast. Over the pristine environment, on the south of the ITCZ, the accumulation mode tends to vanish leading to broad unimodal distributions; the mass loading becomes  $< \sim 70 \text{ mg m}^{-2}$  column. Aerosol size characteristics show an extensive increase in the relative abundance of sub-micron ( $r < 0.5 \mu\text{m}$ ) aerosols in the northern hemisphere. The concentration of these is highest in the coastal and interior regions of the north-western Arabian Sea and decrease rapidly as one moves to the Indian Ocean. The results are discussed based on different aerosol generation mechanisms and the possible transport through air trajectories.

PREVAILING winds transport continental aerosols, generated directly from natural and anthropogenic activities (wind blown mineral dust, industrial and urban effluvia) and indirectly from gas phase reactions of anthropogenic low volatile vapours in the atmosphere, over to oceanic environments. Such aerosol transport is a major perturbing component of the marine aerosol system<sup>1-5</sup>. Impact of aerosol components of possible continental origin in influencing physical and optical properties of pure oceanic aerosols have been reported by various researchers<sup>5-7</sup>. The inter-tropical convergence zone (ITCZ) is a region where the two opposing flows, one from the northern continents and the other from southern pristine ocean, meet causing a convergence and deep convection. The

seasonal movement of the ITCZ causes the polluted continental air to overlap with the purer oceanic environment during favourable seasons (the Indian winter, for example); such movement cleanses the continental air, but also pollutes the oceanic air<sup>7,8</sup>. The finer aerosols (or the sub-micron aerosols), which are mainly generated over the land by gas phase reactions of industrial and urban effluents (mainly sulphates, and nitrates and soot), contribute significantly to pollution because of their longer residence time in the atmosphere<sup>2,9</sup>. One of the objectives of the INDOEX programme is to assess the role of these continental aerosols in modifying the features of the marine boundary layer (MBL) and the role of ITCZ in transporting them horizontally and vertically<sup>8</sup>. In this paper, we present an investigation of the changes in aerosol size distributions and number concentrations over the Arabian Sea and the Indian Ocean and their relation to the ITCZ; the data come from on board measurements from the cruise # 133 of *Sagar Kanya* during the First Field Phase (FFP-98) of the INDOEX.

## Basic data

The basic data used for this study are the aerosol spectral optical depth ( $\tau_{p\lambda}$ ) obtained at 10 narrow wavelength bands using a multiwavelength radiometer (MWR) on-board the cruise, at various oceanic locations. The details of the cruise track, instruments, the wavelengths involved and estimation of  $\tau_{p\lambda}$  are described in another paper in this issue<sup>10</sup>. In all, 14 sets of  $\tau_{p\lambda}$  estimates are made on 14 clear days between 25 February 1998 and 28 March 1998, at 14 distinct locations over the Arabian Sea and south-west Indian Ocean on either side of the ITCZ. The distribution of these data samples are given in Table 1, where the entire data are put into three groups G-I, G-II and G-III; G-I and G-II pertaining to the oceanic regions north of the ITCZ and G-III to the pristine environment south of the ITCZ. G-I contains data collected during the onward leg, mainly along the coastal Arabian Sea and equatorial Indian Ocean closer to the Indian peninsula, while G-II contains data from the same oceanic regions, but much farther away from the peninsula, during the return leg of

<sup>§</sup>For correspondence. (e-mail: spl\_vssc@vssc.org)